Biogeosciences Discuss., https://doi.org/10.5194/bg-2018-210
Manuscript under review for journal Biogeosciences
Discussion started: 15 May 2018

Biogeosciences Discussions Open Access EGU

Distributions of ^{210}Po and ^{210}Pb activities along the North Atlantic GEOTRACES GA01 (GEOVIDE) cruise: partitioning between the particulate and dissolved phase

Yi Tang[1,2], Maxi Castrillejo[3,4], Montserrat Roca-Martí[3], Pere Masqué[3,5], Nolwenn Lemaitre[6], Gillian Stewart[2,1]

[1] Department of Earth and Environmental Sciences, the Graduate Center, City University of New York, New York, USA
[2] School of Earth and Environmental Sciences, Queens College, City University of New York, Flushing, USA
[3] Institut de Ciència i Tecnologia Ambientals & Departament de Física, Universitat Autònoma de Barcelona, Bellaterra, 08193, Spain
[4] Laboratory of Ion Beam Physics, ETH-Zürich, Otto-Stern-Weg 5, Zürich, 8093, Switzerland
[5] School of Science and Centre for Marine Ecosystems Research, Edith Cowan University, Joondalup, Western Australia, Australia
[6] Department of Earth Sciences, Institute of Geochemistry and Petrology, ETH-Zürich, Zürich, Switzerland
Correspondence to: Gillian Stewart (Gillian.Stewart@qc.cuny.edu)

Biogeosciences Discuss., https://doi.org/10.5194/bg-2018-210
Manuscript under review for journal Biogeosciences
Discussion started: 15 May 2018

Abstract

Vertical distributions of total and particulate ^{210}Po and ^{210}Pb activities in the water column were measured at eleven stations in the North Atlantic during the GEOTRACES GA01 GEOVIDE cruise in May - June 2014. Total ^{210}Po activity was on average 24% lower than ^{210}Pb activity in the upper 100 m, and was closer to unity in the mesopelagic (100 – 1000 m). The partitioning coefficients (K_d) along the transect suggest the preferential association of ^{210}Po relative to ^{210}Pb onto particles. The prominent role of small particles in sorption was confirmed by the observation that over 80% of the particulate radionuclide activity was on small particles. To account for the observed surface water ^{210}Po/^{210}Pb disequilibria, particulate radionuclide activities and export of both small (1-53 μm) and large (> 53 μm) particles must be considered. A comparison between the GEOVIDE total particulate ^{210}Po/^{210}Pb activity ratios (AR) and the ratios in previous studies revealed a distinct geographic distribution, with lower particulate AR in the high-latitude North Atlantic (including this study) and Arctic in relation to all other samples. For the samples where apparent oxygen utilization (AOU) was calculated at the same depth and time as the ^{210}Po/^{210}Pb AR (40 stations including this study), there was a two-phase correlation between the total particulate AR and AOU demonstrating the competing forces of remineralization and radionuclide decay from particles as they age.

Biogeosciences Discuss., https://doi.org/10.5194/bg-2018-210
Manuscript under review for journal Biogeosciences
Discussion started: 15 May 2018

1 Introduction

The major goal of the international GEOTRACES program is to characterize the distributions of trace elements and isotopes (TEIs) in the ocean on a global scale, and to identify and quantify processes that control these distributions (GEOTRACES Planning Group, 2006). The GEOVIDE section was a contribution of the French GEOTRACES program to this global survey in the North Atlantic. The GEOVIDE GA01 cruise was carried out in 2014 in the North Atlantic at latitudes greater than 40 ºN and consisted of two sections: the seventh repetition of the OVIDE section from Lisbon (Portugal) to Cape Farewell (southeast tip of Greenland), and a Cape Farewell to St. John's (Canada) section across the Labrador Sea (Fig. 1). The water mass properties and main current transports have been well studied in the OVIDE section during six previous repeated hydrological surveys (2002-2012) (García-Ibáñez et al., 2015). Conditions along the Cape Farewell-St. John's section, however, were relatively unknown. The combination of the two sections constitutes a mixture of complex water masses, circulation patterns, and oceanic boundaries, presenting a special opportunity to analyze the rates of the processes that govern the distribution of TEIs.

Polonium-210 (^{210}Po, $T_{1/2}$ = 138.4 d) and its radioactive grandparent Lead-210 (^{210}Pb, $T_{1/2}$ = 22.3 y) are two non-conservative ^{238}U decay series products. The GEOTRACES program has included both radionuclides in its TEIs list primarily due to ^{210}Po's enhanced bioaccumulation and the use of the ^{210}Po/^{210}Pb pair as a proxy for assessing particle export in the upper ocean. The distribution of ^{210}Po and ^{210}Pb has been widely measured over the last several decades in the Atlantic (e.g. Bacon et al., 1976), Pacific (e.g. Nozaki and Tsunogai 1976), Indian (e.g. Subha Anand et al., 2017), Arctic (e.g. Roca-Martí et al., 2016) and Southern Oceans (e.g. Friedrich and Rutgers van der Loeff 2002). However, since the data reported by Bacon et al. (1980b) at the Labrador Sea stations (47.8 – 53.7 °N), there are few studies of ^{210}Po and ^{210}Pb activity in the North Atlantic at latitudes greater than 40 °N. The GEOVIDE cruise, which targeted the North Atlantic from 40 °N to 60 °N, provided an opportunity to fill this data gap.

Besides ascertaining the distribution of the natural radionuclides under specific geographic conditions, this project aimed to answer questions about their biogeochemical behaviors in various marine environments. Owing to the significantly longer half-life of ^{210}Pb relative to ^{210}Po, the two radionuclides are expected to be in secular equilibrium (total ^{210}Po/^{210}Pb activity ratio = 1) in the ocean, assuming no net removal or addition of either radionuclide. A deficit of ^{210}Po activity relative to ^{210}Pb activity (^{210}Po/^{210}Pb activity ratio < 1), however, is commonly found in the upper

Biogeosciences Discuss., https://doi.org/10.5194/bg-2018-210
Manuscript under review for journal Biogeosciences
Discussion started: 15 May 2018

ocean (e.g. Bacon et al., 1976; Nozaki and Tsunogai 1976; Cochran et al., 1983; Sarin et al., 1999). This has been attributed to a higher particle reactivity of ^{210}Po (higher partitioning coefficient, K_d) than ^{210}Pb in seawater. Particles, therefore, become enriched in ^{210}Po (^{210}Po/^{210}Pb activity ratio > 1) and their sinking to deeper waters results in a ^{210}Po activity deficit relative to ^{210}Pb activity in the upper water column where particles are formed.

In this work, we present the distributions of total and particulate ^{210}Po and ^{210}Pb activity at 11 stations along the GEOVIDE cruise. These data are a significant contribution to the high-latitude North Atlantic ^{210}Po and ^{210}Pb activity data set. In addition, we calculate the K_d of ^{210}Po and ^{210}Pb during scavenging, discuss why this value has a complicated interpretation, and is mostly likely driven by sorption to small particles. We also put our somewhat unusually low particulate ^{210}Po/^{210}Pb activity ratios (AR) into a global context and look for any possible cause of variation along the cruise path.

2 Methods

2.1 Sample collection

The French GEOTRACES cruise to the North Atlantic (GEOVIDE, Section GA01; May 15 – June 30, 2014) was completed on the *N/O Pourquoi Pas?*. The research vessel departed from Lisbon, Portugal, headed northwest to the Greenland shelf, crossed the Labrador Sea, and ended in St John's, Newfoundland, Canada (Fig. 1). A rosette equipped with conductivity-temperature-depth sensors and 12 L Niskin bottles was used to collect 200 seawater samples (5 – 10 L each) from 10 full water column "super" stations (16 – 22 depths/station) and 1 "Xlarge" station to 800 m (station 26, 9 depths) for the determination of total ^{210}Po and ^{210}Pb activity. Upon recovery, seawater samples were transferred to 10 L acid-cleaned containers. In addition, particulate radionuclide activities in two size classes (1-53 µm and > 53 µm) were collected at 3 – 10 depths per station using large volume *in-situ* filtration systems (Challenger Oceanic pumps and McLane pumps) equipped with 142 mm filter holders. Each filter head contained a stacked 53 µm PETEX screen followed by a 1 µm pore size quartz fiber QMA filter. The volume filtered was determined via flow meters mounted below each filter head, and the mean volume pumped through each head was 881 L. Once recovered, clear polyethylene caps were placed on the top of the pump heads and they were brought into a clean laboratory for sub-sampling.

Biogeosciences Discuss., https://doi.org/10.5194/bg-2018-210
Manuscript under review for journal Biogeosciences
Discussion started: 15 May 2018

98 **2.2 Total ^{210}Po and ^{210}Pb**

99 Total ^{210}Po and ^{210}Pb activities were determined from the seawater samples by the cobalt-
100 ammonium pyrrolidine dithiocarbamate (Co-APDC) technique (Fleer and Bacon 1984). Samples
101 were acidified to a pH < 2 with concentrated HCl immediately after collection and spiked with
102 known amounts of ^{209}Po and stable lead as chemical yield tracers. After vigorous stirring and at
103 least 6 h of isotope equilibration, cobalt nitrate and APDC solutions were added to co-precipitate
104 Po and Pb. Samples were filtered through a 0.45 μm membrane filter and transferred into a clean
105 bottle, sealed with parafilm, and stored in double-bags. Further sample processing and analyses
106 were split between the Laboratori de Radioactivitat Ambiental (LRA) at Universitat Autònoma de
107 Barcelona (UAB) (samples from stations 1, 13, and 21) and the Stewart laboratory at Queens
108 College (QC) (stations 26, 32, 38, 44, 60, 69, and 77) to ensure higher counting statistics in the
109 samples. Both laboratories followed the same procedure. Briefly, the filters were digested in a
110 mixture of concentrated HNO_3 and HCl, evaporated to dryness, and eventually dissolved in 1M
111 and 0.5 M HCl at UAB and QC, respectively. A polished pure silver disc (Flynn 1968) with one
112 side covered by enamel paint was placed into the weak acid solution and heated so that the nuclides
113 were spontaneously plated onto only one side of the disc. The activities of both Po nuclides on the
114 disc were measured by alpha spectrometry. Any ^{210}Po and ^{209}Po remaining in the plating solution
115 was removed using AG 1-X8 anion exchange resin and the final solution was re-spiked with ^{209}Po
116 and stored for more than 6 months to allow ingrowth of ^{210}Po from the decay of ^{210}Pb.
117 The ^{210}Pb activity was then determined by re-plating the solutions using silver discs and
118 measuring the ingrown ^{210}Po. Two aliquots of the plating solutions for each sample were taken
119 before the first and second platings for the measurement of total Pb concentration by inductively
120 coupled plasma mass spectrometry (ICP-MS) to determine sample recovery during processing.
121 The average recoveries produced by the LRA and Stewart groups were 83 ± 11% (n = 54) and 76
122 ± 14% (n = 144), respectively. Finally, the initial activities of ^{210}Po and ^{210}Pb at the time of
123 collection were determined by a series of corrections, including nuclide decay, ingrowth, chemical
124 recoveries, detector backgrounds, and blank contamination following the methods in Rigaud et al.
125 (2013). The activity uncertainties from LRA were on average 8% for both ^{210}Po and ^{210}Pb activity,
126 while the activity uncertainties from the Stewart group were on average 13% for ^{210}Po activity and
127 16% for ^{210}Pb activity.
128

Biogeosciences Discuss., https://doi.org/10.5194/bg-2018-210
Manuscript under review for journal Biogeosciences
Discussion started: 15 May 2018

129 **2.3 Particulate ^{210}Po and ^{210}Pb**

130 After collection via in situ pumping, one quarter (equivalent to ~ 220 L) of the PETEX screen
131 containing > 53 µm or "large" particles was processed for radionuclide activity. Swimmers were
132 carefully removed from all samples. The QMA filters containing 1-53 µm or "small" particles
133 were sub-sampled (2 – 4 punches of 12 mm-diameter) achieving a mean effective volume of ~ 66
134 L. The screens and punches were stored in double-bags at -80 °C until the analyses onshore. The
135 particulate samples were split between the two laboratories in parallel to the seawater samples.
136 The filters were spiked with ^{209}Po tracer solution and stable lead, digested using a mixture of
137 concentrated HF, HNO_3 and HCl at UAB, but only HNO_3 and HCl at QC. After multiple rounds
138 of digestion and evaporation to near dryness, the samples were recovered in 0.5 M HCl solution.
139 Any remaining pieces of filter which were not completely digested were carefully removed, rinsed
140 with 0.5 M HCl solution several times, and then discarded. The analyses of the particulate
141 radionuclide activities were identical to those for the seawater samples described in section 2.2.
142
143 **2.4 Concentration of suspended particulate matter (SPM)**
144 The Planquette group utilized the material on the balance of the screens and filters after
145 subsampling for radionuclides to determine major phase composition (particulate organic matter
146 (POM), lithogenic material, calcium carbonate ($CaCO_3$), opal, $Fe(OH)_3$, and MnO_2) (references
147 therein Lam et al., 2015). The complete details of sampling and analyses will be described in a
148 separate manuscript (Lemaitre et al., in prep.), but the mass concentration of total SPM was
149 calculated as the sum of the chemical dry weight of the major particulate phases.
150 The calculated SPM concentration was compared to the *in-situ* transmission data obtained from
151 the rosette CTD sensor (Fig. S1). The overall negative relationship was statistically significant (R^2
152 = 0.7, n = 53, $p < 0.0001$), suggesting that the SPM concentrations determined were reasonable
153 estimates of particle concentration in the water column. We used the SPM values to determine the
154 partitioning coefficient, K_d, for ^{210}Po and ^{210}Pb in section 4.4.
155
156 **2.5 Primary production**
157 Daily primary production (PP) at each station was determined using the ^{13}C labeling technique
158 by the Dehairs group. The details of sampling and analysis for PP is presented in depth elsewhere
159 (Fonseca-Batista et al., in review). Briefly, seawater samples (3 – 6 depths/station) were collected

from the surface to the depth of 0.2% photosynthetically active radiation (PAR). The seawater was then incubated on deck for 24 h under conditions of photometric depths. After incubation, seawater was filtered through GF/F filters (0.7 µm porosity), followed by ^{13}C determination using elemental analysis-isotope ratio mass spectrometry. Daily PP was derived from the depth-integrated ^{13}C uptake rates.

2.6 Satellite-based data

The 8-day composites of surface chlorophyll-a concentration for each station were retrieved from NASA's MODIS products (https://oceancolor.gsfc.nasa.gov) for the period from January to July 2014. The time-series chlorophyll-a concentrations were used to show the development of a phytoplankton bloom over time along the transect.

2.7 Apparent oxygen utilization and historical values

We compared the GEOVIDE data (particulate radionuclide activity and apparent oxygen utilization) to historical databases and publications. The apparent oxygen utilization (AOU, µmol kg^{-1}), a measurement of respiration and water mass age (Stanley et al., 2012), can be derived from hydrological parameters (pressure, temperature, salinity, and dissolved oxygen) using the built-in function in Ocean Data View. The location, date, database address or publication name, and type of data (particulate ^{210}Po and ^{210}Pb activity or hydrological parameters) from all other studies is listed in the supplemental Table S1.

2.8 Statistical analyses

Statistical analyses were carried out in R Studio version 3 using Fitting Linear Models, and Welch Two Sample t-tests. Linear regression analysis was used to investigate the relationship between total particulate $^{210}Po/^{210}Pb$ AR and AOU. The Welch Two Sample t-test was applied to assess whether the mean of the total particulate $^{210}Po/^{210}Pb$ AR was the same as the mean of the small particulate $^{210}Po/^{210}Pb$ AR. It was also applied to investigate the means of the total ^{210}Pb activity in the western and eastern sections along the transect.

3 Results

3.1 Total ^{210}Po and ^{210}Pb activities

Total ^{210}Po activities ($^{210}Po_t$) in all samples ranged from 2.2 to 16.4 dpm 100 L^{-1} and the mean $^{210}Po_t$ for all samples was 8.8 ± 2.4 dpm 100 L^{-1} (n = 198, Fig. 2). The corresponding total ^{210}Pb activities ($^{210}Pb_t$) were between 2.1 and 20.6 dpm 100L^{-1} with a mean value of 10.0 ± 3.0 dpm 100 L^{-1} (n = 198).

The mean $^{210}Po_t/^{210}Pb_t$ activity ratio (AR) of all samples was 0.92 ± 0.28 (Fig. 2, n = 198). When considering different basins separately, there is a tendency of decreasing $^{210}Po_t/^{210}Pb_t$ AR from the Western European Basin (1.10 ± 0.35) westwards to the Iceland Basin (0.90 ± 0.19) and the Irminger Sea and the Labrador Sea (0.80 ± 0.18 and 0.83 ± 0.21, respectively). For all regions, within the mixed layer and euphotic zone (15 – 47 m), significant deficits of $^{210}Po_t$ (0.80 ± 0.20, n = 40) were observed (Fig. 3). $^{210}Po_t$ had enrichments below the surface at some depths at stations 1, 13, and 21 (Fig. 2) where the sub-surface $^{210}Po_t$ excesses were much larger than the surface depletion. In the depth below the surface to ~ 1500 m in the Iceland Basin, the Irminger Sea, and the Labrador Sea, the water samples still indicated a ^{210}Po deficiency (0.84 ± 0.17, n = 27). Secular equilibrium was generally reached near the bottom depths in all basins except at stations 13 and 60 where the water samples were enriched ($^{210}Po_t/^{210}Pb_t$ AR = 1.58 ± 0.16) and depleted ($^{210}Po_t/^{210}Pb_t$ AR = 0.50 ± 0.12) in $^{210}Po_t$, respectively. Secular equilibrium was also observed at some shallow depths (i.e. 80 m at station 44) and even in surface waters (i.e. 15 m at station 38).

3.2 Particulate ^{210}Po and ^{210}Pb activities

Small particulate ^{210}Po ($^{210}Po_s$) activities varied in a wide range from 0.08 to 4.82 dpm 100L^{-1} (mean: 0.76 ± 0.63 dpm 100L^{-1}, n = 81), about 83% of the values in the small particles were lower than 1.0 dpm 100L^{-1} with higher $^{210}Po_s$ values generally observed in the surface samples (Table S2). The range of small particulate ^{210}Pb ($^{210}Pb_s$) activities was 0.07 to 2.89 dpm 100L^{-1} (mean: 0.56 ± 0.46 dpm 100L^{-1}, n = 81). The vertical profiles of $^{210}Pb_s$ were generally similar to those of $^{210}Po_s$, with relatively high activity in the surface, lower activity in the subsurface and increasing activity with depth. This has been seen in the North Atlantic along the GEOTRACES GA03 transect (Rigaud et al., 2015). The mean $^{210}Po_s/^{210}Pb_s$ activity ratio (AR) was 1.43 ± 0.96 in the surface waters (n = 14, ≤ 47 m), and 1.57 ± 0.90 with all samples included (n = 81, 8 – 3440 m). While most surface observations had an AR of $^{210}Po_s/^{210}Pb_s$ higher than unity, 5 surface samples at stations 69 and 77 showed an enrichment of ^{210}Pb activity over ^{210}Po ($^{210}Po_s/^{210}Pb_s$ AR: 0.62 ± 0.18).

Large particulate ^{210}Po ($^{210}Po_l$) activities ranged from 0.01 to 0.83 dpm $100L^{-1}$ with a mean of 0.10 ± 0.12 dpm $100L^{-1}$ (n = 59, Table S2). The range of ^{210}Pb activity in the large particles ($^{210}Pb_l$) was from 0.02 to 0.67 dpm $100L^{-1}$ (mean: 0.12 ± 0.14 dpm $100L^{-1}$, n = 59). The highest $^{210}Po_l$ and $^{210}Pb_l$ values were found at 30 m at station 26. The mean $^{210}Po_l/^{210}Pb_l$ activity ratio (AR) was 1.09 ± 1.54 in the surface waters (n = 14, ≤ 47 m), and 1.06 ± 0.86 when all data were considered (n = 59, 8-800 m). There were 17% of the samples with a depletion of ^{210}Po activity relative to ^{210}Pb activity in large particles (mean AR: 0.49 ± 0.23), particularly in surface waters from the western section. We address this issue further in section 4.3.

The percentages of total ^{210}Po activity in the small and large particles ranged from 0.9 to 46.7% (mean: 8.0 ± 6.7%) and from 0.1 to 8.9% (mean: 1.2 ± 1.5%), respectively. The percentage of total ^{210}Pb activity ranged from 0.7 to 21.4% (mean: 4.9 ± 3.8%) and from 0.2 to 5.9% (mean: 1.1 ± 1.2%) in the small and large particulate phase, respectively. These values revealed that both radionuclides were predominantly present in the dissolved phase along this transect, as is commonly found in the ocean. The particulate percentages reported here are similar to the values reported from the F.S. "Meteor" cruise 32 in the North Atlantic (Bacon et al., 1976) and along the North Atlantic GA03 transect (Rigaud et al., 2015).

We then combined radionuclide activity on the small and large particles from the same depth as the total particulate activity. There were 56 samples in total (surface to 800 m) and 41 of them were from the upper 200 m. Most of the total particulate ^{210}Po ($^{210}Po_p$) and ^{210}Pb ($^{210}Pb_p$) activity was on the small particles, with 86% of $^{210}Po_p$ and 80% of $^{210}Pb_p$ on the small size fraction (data not shown). The total particulate ^{210}Po and ^{210}Pb AR ($^{210}Po_p/^{210}Pb_p$) had the same mean as that of the small particulate ^{210}Po and ^{210}Pb AR ($^{210}Po_s/^{210}Pb_s$) (Welch Two Sample t-test, n = 56, $p = 0.1$), indicating that the values of the $^{210}Po_p/^{210}Pb_p$ activity ratios were driven by the small particles. While the majority of particulate matter was enriched in ^{210}Po ($^{210}Po_p/^{210}Pb_p$ AR> 1), there were some surface samples that were depleted in ^{210}Po relative to ^{210}Pb. The $^{210}Po_p/^{210}Pb_p$ activity ratios from this study are compared to the results from previous studies in various oceanic regimes in section 4.2.

4 Discussion

4.1 Total ^{210}Po and ^{210}Pb activities

Biogeosciences Discuss., https://doi.org/10.5194/bg-2018-210
Manuscript under review for journal Biogeosciences
Discussion started: 15 May 2018

252 The overall profiles of $^{210}Po_t$ and $^{210}Pb_t$ activities were different among basins (Fig. 2). The
253 deficiencies of $^{210}Po_t$ activities with respect to $^{210}Pb_t$ activities in the surface samples from the
254 Iceland Basin, the Irminger Sea, and the Labrador Sea were generally greater than those from the
255 Western European Basin. Such disequilibria generally extended to the deep waters (1700 – 2950
256 m). In contrast, $^{210}Po_t$ activities in the Western European Basin were generally enriched relative to
257 $^{210}Pb_t$ activities from below the surface to the bottom of the profile. In the Western European Basin,
258 the sub-surface $^{210}Po_t$ activity excess was much larger than the surface depletion, suggesting that
259 some external source would be needed to maintain this excess ^{210}Po activity within the water
260 column. One possible source of these sub-surface ^{210}Po activity excesses could be the eastern
261 boundary upwelling along the coast of the Iberian Peninsula (García-Ibáñez et al., 2015). Even
262 though no strong upwelling events were revealed from temperature and density profiles during the
263 cruise, northerly winds favoring upwelling were recorded 2 – 3 months before the sampling
264 (Shelley et al., 2017). The deep water may have excess ^{210}Po activity due to the remineralization
265 of sinking particles. The upwelling of this water mass prior to the sampling date could maintain
266 excess ^{210}Po activity in the water column if the previous export of ^{210}Po activity was large enough.
267 Similar findings have been reported in the Cariaco Trench by Bacon et al. (1980a).
268 As atmospheric deposition is the main source of ^{210}Pb to the water column (e.g. Masqué et al.,
269 2002), we divided the GA01 transect into a western section (stn. 44 – 77) and an eastern section
270 (stn. 1 - 38) based on atmospheric deposition boxes described in (Shelley et al., 2017). Total
271 atmospheric deposition fluxes of a suite of aerosol-sourced trace metals were all reported to be
272 higher in the east than the west (Shelley et al., 2017). However, a two sample t-test revealed a
273 greater mean of $^{210}Pb_t$ activity in surface waters in the western than in the eastern section ($p < 0.02$,
274 mean: 12.1 vs. 10.4 dpm 100 L^{-1}), despite the fact that ^{210}Pb is usually associated with aerosols.
275 Even though the direct input of atmospheric ^{210}Pb may be larger in the east (assuming it behaves
276 like the other trace metals, but without aerosol ^{210}Pb data we cannot confirm this), alternative
277 inputs of ^{210}Pb from freshwater (e.g., sea ice processes and meteoric water) could be a greater
278 source of ^{210}Pb activity to the west. The freshwater sources over the Greenland shelf and slope
279 have been identified by Benetti et al. (2017), and were believed to be an important source of Fe
280 (Tonnard et al., in review) and Al (Menzel-Barraqueta et al., in review) off of Greenland during
281 this cruise. This unexpected result highlights the need in the future to measure ^{210}Pb activity

Biogeosciences Discuss., https://doi.org/10.5194/bg-2018-210
Manuscript under review for journal Biogeosciences
Discussion started: 15 May 2018

simultaneously in the atmospheric and local freshwater sources in order to account for all source terms.

4.2 Total particulate $^{210}Po/^{210}Pb$ AR

A proposed explanation for the depletion of ^{210}Po activity relative to ^{210}Pb activity (AR <1) in some particles is effective recycling, commonly characterized by a subsurface excess of dissolved ^{210}Po activity released from enriched particles leaving the surface. Bacon et al. (1976) suggested that the efficiency of this recycling could reach up to 50%, while there is no significant concurrent release of ^{210}Pb activity in the water column. Laboratory studies have found the release rate of ^{210}Po in marine particulate matter to be significant; for example, 41% of the ^{210}Po activity in euphausiid fecal pellets was released over 5 days as presented in Heyraud et al. (1976). An alternative explanation for the depletion of ^{210}Po activity in particles is their lithogenic origin. $^{210}Po/^{210}Pb$ AR in lithogenic particles was reported to be similar to or less than unity (Nozaki et al., 1998; Tateda et al., 2003). The AR < 1 observed at station 1 (120, 250, and 550 m) could be associated with lithogenic particles from the Iberian Margin where the lithogenic contribution to particulate and dissolved Fe and dissolved Al were reported to be significant (Gourain et al., in review; Menzel-Barraqueta et al., in review).

The time-series chlorophyll-a concentration (8-day composite, https://oceancolor.gsfc.nasa.gov) from January to July 2014 at each station revealed bloom conditions about 4 months prior to the sampling time (Fig. 4). We estimated the days since the last bloom began prior to the sampling date for each station (Table 1) and put these data into the context of the low $^{210}Po_p/^{210}Pb_p$ AR (< 1) in the total particles > 1 μm. Eight stations had total particulate samples with $^{210}Po_p/^{210}Pb_p$ AR lower than unity from either shallow or deep waters. Specifically, when the time since the last bloom began was relatively short (24 – 47 d) the samples with $^{210}Po_p/^{210}Pb_p$ AR < 1 were observed in the shallow waters (10 – 60 m). In contrast, as longer time (50 – 74 d) passed since the last bloom, the depths at which samples had $^{210}Po_p/^{210}Pb_p$ AR < 1 were found to be much deeper (120 – 500 m). The results indicated that post-bloom particles could be recycled for weeks in shallow depths and take weeks to months to sink to deeper waters.

The averages of $^{210}Po_p/^{210}Pb_p$ AR within the upper 200 m water column were put into a global context with previously reported results (Fig. 5). Total particulate $^{210}Po/^{210}Pb$ AR in the open ocean in previous studies (e.g., Equatorial/western Pacific, Bellingshausen Sea, BATS, Labrador Sea)

were generally greater than unity. In contrast to the open ocean, the data show a distinct trend of depletion of relative ^{210}Po activity in marine particles from the shallow seas of the high latitude northern hemisphere. The lowest total particulate ^{210}Po/^{210}Pb AR values (Table 2, 0.4 – 0.5) were found in the central Arctic and Chukchi shelf (Friedrich 2011; He et al., 2015). Previous studies have observed depletion of relative ^{210}Po activity in nearshore particles in the Yellow Sea (Hong et al., 1999), in the turbid waters off of western Taiwan (Wei et al., 2012), on the shelf of Woods Hole, MA (Rigaud et al., 2015), and now in the margin station off St. John's, Canada (this study). The previous authors attributed the relative depletion of particulate ^{210}Po activity in the nearshore waters to the terrestrial origin/riverine input of particles with a low ^{210}Po/^{210}Pb AR. This may partially explain low activity ratios in the samples from the shelf of the Arctic Ocean as well, since it receives ~ 10% of global river runoff and is the most riverine-influenced of all of the world's oceans (Opsahl et al., 1999; Carmack et al., 2006). The Arctic Basin, similarly, had wide spread deficits of particulate ^{210}Po activity in the upper water column during the sea-ice minimum in 2007 (Roca-Marti et al., in prep.). The author suggested other particle types could also play a role in lowering the particulate AR, including sea-ice sediments, remineralized material, fecal pellets, and picoplankton aggregates.

4.3 Relationship between total particulate ^{210}Po/^{210}Pb AR and AOU

Apparent oxygen utilization (AOU = $O_{2\ saturation} - O_{2\ measured}$), the amount of oxygen that has been consumed by remineralization of exported organic matter in the water column, can be used to indicate the intensity of particle recycling (Ito et al., 2004; Duteil et al., 2013). While AOU is generated both by water mass ageing and concomitant biological oxygen consumption (e.g. Ito et al., 2004; Sonnerup et al., 2015), the two components of AOU would be predicted to have opposite impacts on the $^{210}Po_p/^{210}Pb_p$ AR value. For example, old particles would tend to have a higher $^{210}Po_p/^{210}Pb_p$ activity ratio (closer to 1) because particulate ^{210}Po activity would increase from the decay of ^{210}Pb within mineral lattices and trend towards secular equilibrium ($^{210}Po_p/^{210}Pb_p$ AR = 1). In contrast, oxygen consumption due to bacterial remineralization would preferentially release ^{210}Po activity from particles into the dissolved pool (e.g. Stewart et al., 2008), leading to a lower $^{210}Po_p/^{210}Pb_p$ AR in those particles.

The combination of average $^{210}Po_p/^{210}Pb_p$ AR and their corresponding average AOU in the upper 200 m at 40 stations from 4 independent studies, including ARK-XXII/2 (77.38 – 87.83 ºN,

n = 15) in the Arctic, BOFS (48.89 – 49.87 ºN, n = 7), GA03 (22.38 – 39.70 ºN, n = 7), and GA01 (this study, 40.33 – 59.80 ºN, n = 11) in the North Atlantic (see map in Fig. 5) suggests two distinct linear trends (Fig. 6). When AOU was lower than 25 µmol kg^{-1}, the $^{210}Po_p/^{210}Pb_p$ AR was found to be greater than unity, together with a linear negative relationship (n = 27, R^2 = 0.5, p < 0.001) towards the AOU at 25 µmol kg^{-1}. In contrast, AOU values greater than 25 µmol kg^{-1} were coincident with a $^{210}Po_p/^{210}Pb_p$ AR < 1, and there was a linear positive relationship (n = 12, R^2 = 0.4, p = 0.03) towards the highest AOU values measured. The two contradictory linear trends likely reflect the opposite impacts of the two components (water mass aging and remineralization) of AOU on $^{210}Po_p/^{210}Pb_p$ AR. This suggests that the variation in the $^{210}Po_p/^{210}Pb_p$ AR was mainly driven by remineralization processes under the condition of AOU < 25 µmol kg^{-1}, lowering the total particulate activity ratio; whereas the decay of ^{210}Pb into ^{210}Po towards secular equilibrium may dominate when AOU was > 25 µmol kg^{-1}, leading to an increase in $^{210}Po_p/^{210}Pb_p$ AR. This explanation, however, appears to only hold for the high latitude Northern Hemisphere where $^{210}Po_p/^{210}Pb_p$ activity ratios were generally lower than those in the other oceanic settings (Fig. 5). In the high latitude Southern Hemisphere near Antarctic (e.g., ANT-X/6), for example, there is no apparent relationship between $^{210}Po_p/^{210}Pb_p$ activity ratios and AOU. This relationship (or lack thereof) deserves more study in the future.

4.4 Small particles, sorption, and calculating POC export

The assumption that the largest particles dominate export in the ocean (e.g. Bishop et al., 1977; Fowler and Knauer 1986; Michaels and Silver 1988; Honjo et al., 1992; Walsh and Gardner 1992) has been challenged by increasing studies which argue that small particles can form aggregates that sink, and their contribution to carbon export could be larger than previously thought (e.g. Richardson and Jackson 2007; Lomas and Moran 2011; Amacher et al., 2013; Puigcorbé et al., 2015).

We investigated the role of small phytoplankton to carbon export along the GA01 transect via investigation of pigments and *in-situ* primary production. The fraction of pigment-based size classes suggested a significant contribution of small particles (nano-phytoplankton: 2 – 20 µm 60%, pico-phytoplankton: < 2 µm, 13%) to primary production in the eastern section while larger particles (micro-phytoplankton: > 20 µm, 60%) may have dominated production in the western section of the GA01 transect (Tonnard et al., in prep.). The rate of primary production in the eastern

375 section (mean: 99 ± 50 mmol C m^{-2} d^{-1}), however, was similar to that in the west (mean: 93 ± 58
376 mmol C m^{-2} d^{-1}) (data not shown). While we do not have direct evidence of small particles sinking,
377 we are making an assumption that our study sites behave as the above cited papers have seen
378 elsewhere. Therefore, a possible link between small particles and production, and possibly export
379 (proportional to their role in production according to Richardson and Jackson, 2007), may exist
380 along the transect.

381 The partitioning coefficient, K_d (L kg^{-1}), has been used to describe the particle adsorption
382 behavior of radionuclides. It is defined as the ratio of the adsorbed radionuclide activity (A_p, dpm
383 $100L^{-1}$) to the dissolved radionuclide activity (A_d, dpm $100L^{-1}$), normalized by the suspended
384 particulate matter concentration (SPM, µg L^{-1}):

385 $$K_d = \frac{A_p}{A_d} \times \frac{1}{SPM} 10^9 \qquad (1)$$

386 Owing to the different biological and chemical behaviors of ^{210}Po and ^{210}Pb, the interpretation
387 of measured K_d for ^{210}Po (K_d(Po)) may not be as clear as that for ^{210}Pb (K_d(Pb)) (i.e. K_d(Po) also
388 takes the fraction of absorbed ^{210}Po into account, Tang et al., 2017). As such, it would be more
389 appropriate to think of both K_d(Po) and K_d(Pb) as the intensity parameter for the radionuclide
390 association with particles.

391 In this study, the size-fractionated data of radionuclide activity and SPM allowed us to
392 calculate the partitioning coefficients for both radionuclides on small and large particles. We
393 present only the coefficients for the small particulate phases ($K_d(Po)_s$, $K_d(Pb)_s$) and the total
394 particulate phases ($K_d(Po)_p$, $K_d(Pb)_p$) because most of the particulate activity (> 80%) was
395 associated with the small particles along the GEOVIDE transect, and most conceptualized
396 scavenging models consider either the two-box model (dissolved – total particulate phases, i.e.
397 $K_d(Po)_p$) or the three-box model (dissolved – small – large, i.e. $K_d(Po)_s$) (Clegg and Whitfield 1990;
398 1991; Rigaud et al., 2015) and thus activity is concentrated from the dissolved phase to the total
399 or small particles. The K_d values for the small particulate phase were slightly higher than those for
400 the total particulate phase but overall these values were very similar for both radionuclides (Fig.
401 7). Combining the fact that adsorption/scavenging was in fact driven by small particles with the
402 contribution of small phytoplankton to production, the importance of small particles to
403 radionuclide export is suggested. We recommend combining the activities of both small and large
404 particles into a total particulate fraction in order to explain total ^{210}Po/^{210}Pb disequilibria in the

surface waters, and utilizing the characteristics of the total particles (instead of just the large particles) in the estimation of the POC export fluxes (Tang et al., in prep.).

5 Conclusions

In this study, we reported the vertical distribution of total and size-fractionated particulate ^{210}Po and ^{210}Pb activities in the North Atlantic during the GEOVIDE GA01 cruise. More than 90% of the radionuclide activity was found in the dissolved phase, while a small proportion was associated with particles in this transect. Total ^{210}Po activity was generally depleted relative to total ^{210}Pb activity in the upper 100 m due to the assumed preferential adsorption and uptake of ^{210}Po activity by particles.

Over 80% of the particulate radionuclide activity was on small particles, and it appeared that the adsorption/scavenging of both radionuclides was driven by small particles. Considering this and the contributions of small phytoplankton to primary production (and possibly export), we suggest combining the activities of both ^{210}Po and ^{210}Pb from both small and large particles into a total particulate fraction (> 1 μm) in order to explain the water column ^{210}Po/^{210}Pb disequilibria and calculate POC export.

There appear to be geographic differences in particulate ^{210}Po/^{210}Pb activity ratios measured during GEOVIDE and previous studies, with particularly low values in the high-latitude North Atlantic and Arctic. While this observation deserves more attention, we support previous suggestions that this is due to the terrestrial origin/riverine input of particles with a low ^{210}Po/^{210}Pb AR into the river-dominated shallow basins of the Arctic. Considering the age of the particles and water masses as well as the importance of remineralization may also explain some of these observations, as there was a significant relationship between the total particulate activity ratio and AOU when both were measured in the high latitude North Atlantic and Arctic Oceans.

Acknowledgements

Thank you to the chief scientists (G. Sarthou and P. Lherminier) of the GEOVIDE cruise, and the captain (G. Ferrand), and crew of the *N/O Pourquoi Pas?* for their support of this work. Many thanks to P. Branellec, F. Desprez de Gésincourt, M. Hamon, C. Kermabon, P. Le Bot, S. Leizour,

O. Ménage, F. Pérault, and E. de Saint-Léger for their technical support during the GEOVIDE expedition, and to C. Schmechtig for the GEOVIDE database management. P. Lam is also acknowledged for providing two modified McLane ISP. Special thanks go to the member of the pump group including F. Planchon, V. Sanial, and C. Jeandel. The author would like to thank C. Mariez, S. Roig, F. Planchon, and H. Planquette who helped in providing particle composition data and A. Roukaerts, D. Fonseca-Batista, F. Deman, and F. Dehairs for primary production data. We also would like to acknowledge the funding agencies: the French National Research Agency (ANR-13-BS06-0014, ANR-12-PDOC-0025-01), the French National Center for Scientific Research (CNRS-LEFE-CYBER), the LabexMER (anr-10-LABX-19), and Ifremer. G. Stewart and Y. Tang were supported by NSF award #OCE 1237108. M. Castrillejo and M. Roca-Marti were funded by an FPU PhD studentship (AP-2012-2901 and AP2010-2510, respectively) from the Ministerio de Educación, Cultura y Deporte of Spain. M. Castrillejo was also supported by the ETH Zurich Postdoctoral Fellowship Program (17-2 FEL-30), co-funded by the Marie Curie Actions for People COFUND Program. Additional thanks go to G. Hemming and T. Rasbury for laboratory assistance with the ICP-MS analyses.

References:

Amacher, J., Neuer, S. and Lomas, M.: DNA-based molecular fingerprinting of eukaryotic protists and cyanobacteria contributing to sinking particle flux at the Bermuda Atlantic time-series study, Deep Sea Research Part II, 93, 71-83, 2013.

Bacon, M. P.: 210Pb and 210Po results from F.S. "Meteor" cruise 32 in the North Atlantic, PANGAEA, 1977.

Bacon, M. P., Belastock, R. A., Tecotzky, M., Turekian, K. K. and Spencer, D. W.: Lead-210 and polonium-210 in ocean water profiles of the continental shelf and slope south of New England, Continental Shelf Research, 8, 841-853, 1988.

Bacon, M. P., Brewer, P. G., Spencer, D. W., Murray, J. W. and Goddard, J.: Lead-210, polonium-210, manganese and iron in the Cariaco Trench, Deep Sea Research Part A. Oceanographic Research Papers, 27, 119-135, 1980a.

Bacon, M. P., Spencer, D. W. and Brewer, P. G.: 210Pb/226Ra and 210Po/210Pb disequilibria in seawater and suspended particulate matter, Earth and Planetary Science Letters, 32, 277-296, 1976.

Bacon, M. P., Spencer, D. W. and Brewer, P. G.: Lead-210 and Polonium-210 as Marine Geochemical Tracers: Review and Discussion of Results from the Labrador Sea, Natural radiation environment III, T. F. Gesell and W. M. Lowder, 1**,** 473-501, 1980b.

Benetti, M., Reverdin, G., Lique, C., Yashayaev, I., Holliday, N. P., Tynan, E., Torres-Valdes, S., Lherminier, P., Tréguer, P. and Sarthou, G.: Composition of freshwater in the spring of 2014 on the southern Labrador shelf and slope, Journal of Geophysical Research: Oceans, 122, 1102-1121, 2017.

Bishop, J. K. B., Edmond, J. M., Ketten, D. R., Bacon, M. P. and Silker, W. B.: The chemistry, biology, and vertical flux of particulate matter from the upper 400 m of the equatorial Atlantic Ocean, Deep Sea Research, 24, 511-548, 1977.

BODC, Lowry, R. K., Machin, P. and Cramer, R. N.: Compilation of the results of EU-project BOFS, PANGAEA, 2016.

Carmack, E., Barber, D., Christensen, J., Macdonald, R., Rudels, B. and Sakshaug, E.: Climate variability and physical forcing of the food webs and the carbon budget on panarctic shelves, Progress in Oceanography, 71, 145-181, 2006.

Clegg, S. L. and Whitfield, M.: A generalised model for the scavenging of trace metals in the open ocean: I. Particle cycling, Deep Sea Research Part A. Oceanographic Research Papers, 37, 809-832, 1990.

Clegg, S. L. and Whitfield, M.: A generalied model for the scavenging of trace metals in the open ocean-II. Thorium scavenging, Deep Sea Research Part A. Oceanographic Research Papers, 38, 91-120, 1991.

Cochran, J. K., Bacon, M. P., Krishnaswami, S. and Turekian, K. K.: 210Po and210Pb distributions in the central and eastern Indian Ocean, Earth and Planetary Science Letters, 65, 433-452, 1983.

Duteil, O., Koeve, W., Oschlies, A., Bianchi, D., Galbraith, E., Kriest, I. and Matear, R.: A novel estimate of ocean oxygen utilisation points to a reduced rate of respiration in the ocean interior, Biogeosciences, 10, 7723-7738, 2013.

Fleer, A. P. and Bacon, M. P.: Determination of 210Pb and 210Po in seawater and marine particulate matter, Nuclear Instruments and Methods in Physics Research, 223, 243-249, 1984.

Flynn, W. W.: The determination of low levels of polonium-210 in environmental materials, Analytica Chimica Acta, 43, 221-227, 1968.

Fonseca-Batista, D., Li, X., Riou, V., Michotey, V., Fripiat, F., Deman, F., Guasco, S., Brion, N., Lemaitre, N., Planchon, F., Tonnard, M., Planquette, H., Gallinari, M., Sarthou, G., Elskens, M., Chou, L. and Dehairs, F.: Evidence of high N2 fixation rates in productive waters of the temperate Northeast Atlantic, Biogeosciences, in review.

Fowler, S. W. and Knauer, G. A.: Role of large particles in the transport of elements and organic compounds through the oceanic water column, Progress in Oceanography, 16, 147-194, 1986.

Friedrich, J.: Polonium-210 and Lead-210 activities measured on 17 water bottle profiles and 50 surface water samples during POLARSTERN cruise ARK-XXII/2, PANGAEA, 2011.

Friedrich, J., Robert, M. and Stimac, I.: Polonium-210 and Lead-210 activities measured on 9 water bottle profiles during POLARSTERN cruise ANT-XXIV/3, PANGAEA, 2011.

Friedrich, J. and Rutgers van der Loeff, M. M.: A two-tracer (210Po–234Th) approach to distinguish organic carbon and biogenic silica export flux in the Antarctic Circumpolar Current, Deep Sea Research Part I: Oceanographic Research Papers, 49, 101-120, 2002.

García-Ibáñez, M. I., Pardo, P. C., Carracedo, L. I., Mercier, H., Lherminier, P., Ríos, A. F. and Pérez, F. F.: Structure, transports and transformations of the water masses in the Atlantic Subpolar Gyre, Progress in Oceanography, 135, 18-36, 2015.

GEOTRACES Planning Group: GEOTRACES Science Plan, Baltimore, Maryland, 2006.

Gourain, A., Planquette, H., Cheize, M., Menzel-Barraqueta, J. L., Boutorh, J., Shelley, R. U., Pereira-Contreira, L., Lemaitre, N., Lacan, F., Lherminier, P. and Sarthou, G.: Particualte trace metals along the GEOVIDE section, Biogeosciences, in review.

He, J., Yu, W., Lin, W., Men, W. and Chen, L.: Particulate organic carbon export fluxes on Chukchi Shelf, western Arctic Ocean, derived from 210Po/210Pb disequilibrium, Chinese Journal of Oceanology and Limnology, 33, 741-747, 2015.

Heyraud, M., Fowler, S. W., Beasley, T. M. and Cherry, R. D.: Polonium-210 in euphausiids: A detailed study, Marine Biology, 34, 127-136, 1976.

Hong, G.-H., Park, S.-K., Baskaran, M., Kim, S.-H., Chung, C.-S. and Lee, S.-H.: Lead-210 and polonium-210 in the winter well-mixed turbid waters in the mouth of the Yellow Sea, Continental Shelf Research, 19, 1049-1064, 1999.

Honjo, S., Spencer, D. W. and Gardner, W. D.: A sediment trap intercomparison experiment in the Panama Basin, 1979, Deep Sea Research Part A. Oceanographic Research Papers, 39, 333-358, 1992.

Hu, W., Chen, M., Yang, W., Zhang, R., Qiu, Y. and Zheng, M.: Enhanced particle scavenging in deep water of the Aleutian Basin revealed by 210Po- 210Pb disequilibria, Journal of Geophysical Research: Oceans, 119, 3235-3248, 2014.

Ito, T., Follows, M. J. and Boyle, E. A.: Is AOU a good measure of respiration in the oceans?, Geophysical Research Letters, 31, 1-4, 2004.

Kim, G. and Church, T. M.: Seasonal biogeochemical fluxes of 234Th and 210Po in the Upper Sargasso Sea: Influence from atmospheric iron deposition, Global Biogeochemcal Cycles, 15, 651-661, 2001.

Lam, P. J., Ohnemus, D. C. and Auro, M. E.: Size-fractionated major particle composition and concentrations from the US GEOTRACES North Atlantic Zonal Transect, Deep Sea Research Part II, 116, 303-320, 2015.

Lemaitre, N., Planquette, H., Planchon, F., Roig, S., Sarthon, G. and Dehairs, F.: High variability of export fluxes along the North Atlantic GEOTRACES section GA01: Importance of minerals as ballast of particulate orgnaic carbon export, in prep.

Lomas, M. W. and Moran, S. B.: Evidence for aggregation and export of cyanobacteria and nano-eukaryotes from the Sargasso Sea euphotic zone, Biogeosciences, 8, 203-216, 2011.

Masqué, P., Sanchez-Cabeza, J. A., Bruach, J. M., Palacios, E. and Canals, M.: Balance and residence times of 210Pb and 210Po in surface waters of the northwestern Mediterranean Sea, Continental Shelf Research, 22, 2127-2146, 2002.

Menzel-Barraqueta, J.-L., Schlosser, C., Planquette, H., Gourain, A., Cheize, M., Boutorh, J., Shelley, R., Contreira, L. P., Gledhill, M., Hopwood, M. J., Lherminier, P., Sarthou, G. and Achterberg, E. P.: Aluminium in the North Atlantic Ocean and the Labrador Sea (GEOTRACES GA01 section): roles of continental inputs and biogenic particle removal, Biogeosciences, in review.

Michaels, A. F. and Silver, M. W.: Primary production, sinking fluxes and the microbial food web, Deep Sea Research Part A. Oceanographic Research Papers, 35, 473-490, 1988.

Moore, R. M. and Smith, J. N.: Disequilibria between226Ra, 210Pb and 210Po in the Arctic Ocean and the implications for chemical modification of the Pacific water inflow, Earth and Planetary Science Letters, 77, 285-292, 1986.

Murray, J. W., Paul, B., Dunne, J. P. and Chapin, T.: 234Th, 210Pb, 210Po and stable Pb in the central equatorial Pacific: Tracers for particle cycling, Deep Sea Research Part I: Oceanographic Research Papers, 52, 2109-2139, 2005.

Nozaki, Y., Dobashi, F., Kato, Y. and Yamamoto, Y.: Distribution of Ra isotopes and the 210Pb and 210Po balance in surface seawaters of the mid Northern Hemisphere, Deep Sea Research Part I: Oceanographic Research Papers, 45, 1263-1284, 1998.

Nozaki, Y. and Tsunogai, S.: 226Ra, 210Pb and 210Po disequilibria in the Western North Pacific, Earth and Planetary Science Letters, 32, 313-321, 1976.

Opsahl, S., Benner, R. and Amon, R. M. W.: Major flux of terrigenous dissolved organic matter through the Arctic Ocean, Limnology and Oceanography, 44, 2017-2023, 1999.

Peck, G. and Smith, J. D.: Uranium decay series radionuclides in the Western Equatorial Pacific Ocean and their use in estimating POC fluxes, J.-M. Fernandez and R. Fichez, Paris, 459-469, 2002.

Puigcorbé, V., Benitez-Nelson, C. R., Masqué, P., Verdeny, E., White, A. E., Popp, B. N., Prahl, F. G. and Lam, P. J.: Small phytoplankton drive high summertime carbon and nutrient export in the Gulf of California and Eastern Tropical North Pacific, Global Biogeochemcal Cycles, 29, 1309-1332, 2015.

Richardson, T. L. and Jackson, G. A.: Small Phytoplankton and Carbon Export from the Surface Ocean, Science, 315, 838-840, 2007.

Rigaud, S., Puigcorbe, V., Camara-Mor, P., Casacuberta, N., Roca-Marti, M., Garcia-Orellana, J., Benitez-Nelson, C. R., Masqué, P. and Church, T.: A methods assessment and recommendations for improving calculations and reducing uncertainties in the determination of 210Po and 210Pb activities in seawater, Limnology and Oceanography Methods, 11, 561-571, 2013.

Rigaud, S., Stewart, G., Baskaran, M., Marsan, D. and Church, T.: 210Po and 210Pb distribution, dissolved-particulate exchange rates, and particulate export along the North Atlantic US GEOTRACES GA03 section, Deep Sea Research Part II, 116, 60-78, 2015.

Roca-Marti, M., Puigcorbe, V., Friedrich, J., Rutgers van der Loeff, M. M., Rabe, B., Korhonen, M., Canara-Mor, P., Garcia-Orellana, J. and Masqué, P.: Distribution of 210Pb and 210Po in the

Arctic water column during 2007 sea-ice minimun: particle export in the ice-covered basins, in prep.

Roca-Martí, M., Puigcorbé, V., Rutgers van der Loeff, M. M., Katlein, C., Fernández-Méndez, M., Peeken, I. and Masqué, P.: Carbon export fluxes and export efficiency in the central Arctic during the record sea-ice minimum in 2012: a joint 234Th/ 238U and 210Po/ 210Pb study, Journal of Geophysical Research: Oceans, 121, 5030-5049, 2016.

Sarin, M. M., Kim, G. and Church, T. M.: 210Po and 210Pb in the South-equatorial Atlantic:, Deep Sea Research Part II, 46, 907-917, 1999.

Shelley, R. U., Roca-Martí, M., Castrillejo, M., Sanial, V., Masqué, P., Landing, W. M., van Beek, P., Planquette, H. and Sarthou, G.: Quantification of trace element atmospheric deposition fluxes to the Atlantic Ocean (>40°N; GEOVIDE, GEOTRACES GA01) during spring 2014, Deep Sea Research Part I: Oceanographic Research Papers, 119, 34-49, 2017.

Shimmield, G. B., Ritchie, G. D. and Fileman, T. W.: The impact of marginal ice zone processes on the distribution of 21OPb, 21OPo and 234Th and implications for new production in the Bellingshausen Sea, Antarctica, Deep Sea Research Part II, 42, 1313-1335, 1995.

Smetacek, V., de Baar, H. J. W., Bathmann, U., Lochte, K. and Rutgers van der Loeff, M. M.: Export production by 234Th, including 210Po and 210Pb measured on water bottle samples during POLARSTERN cruise ANT-X/6, PANGAEA, 1997.

Sonnerup, R. E., Mecking, S., Bullister, J. L. and Warner, M. J.: Transit time distributions and oxygen utilization rates from chlorofluorocarbons and sulfur hexafluoride in the Southeast Pacific Ocean, Journal of Geophysical Research: Oceans, 120, 3761-3776, 2015.

Stanley, R. H. R., Doney, S. C., Jenkins, W. J. and Lott, D. E. I.: Apparent oxygen utilization rates calculated from tritium and helium-3 profiles at the Bermuda Atlantic Time-series Study site, Biogeosciences, 9, 1969-1983, 2012.

Stewart, G., Cochran, J. K., Miquel, J. C., Masqué, P., Szlosek, J., Rodriguez y Baena, A. M., Fowler, S. W., Gasser, B. and Hirschberg, D. J.: Comparing POC export from 234Th/238U and 210Po/210Pb disequilibria with estimates from sediment traps in the northwest Mediterranean, Deep Sea Research Part I: Oceanographic Research Papers, 54, 1549-1570, 2007.

Stewart, G. M., Fowler, S. W. and Fisher, N. S.: Chapter 8 The Bioaccumulation of U- and Th-Series Radionuclides in Marine Organisms, Radioactivity in the Environment. Elsevier, Volume 13**,** 269-305, 2008.

Subha Anand, S., Rengarajan, R., Shenoy, D., Gauns, M. and Naqvi, S. W. A.: POC export fluxes in the Arabian Sea and the Bay of Bengal: A simultaneous 234Th/238U and 210Po/210Pb study, Marine Chemistry, 2017.

677 Tang, Y., Castrillejo, M., Roca-Marti, M., Masqué, P., Lemaitre, N. and Stewart, G.: POC export
678 fluxes and export efficiency along the North Atlantic GEOTRACES GA01 (GEOVIDE) transect
679 estimated from 210Po/210Pb disequilibria, in prep.
680
681 Tang, Y., Stewart, G., Lam, P. J., Rigaud, S. and Church, T.: The influence of particle
682 concentration and composition on the fractionation of 210Po and 210Pb along the North Atlantic
683 GEOTRACES transect GA03, Deep Sea Research Part I: Oceanographic Research Papers, 128,
684 42-54, 2017.
685
686 Tateda, Y., Carvalho, F. P., Fowler, S. W. and Miquel, J.-C.: Fractionation of 210Po and 210Pb in
687 coastal waters of the NW Mediterranean continental margin, Continental Shelf Research, 23, 295-
688 316, 2003.
689
690 Tonnard, M., Donval, A., Lampert, L., Claustre, H., Ras, J., Dimier, C., Sarthou, G., Planquette,
691 H., van der Merwe, P., Boutorh, J., Cheize, M., Menzel, J.-L., Pereira Contraira, L., Shelley, R.,
692 Bowie, A. R., Treguer, P., Gallinari, M., Duprez de Gesincourt, F., Germain, Y. and Leherminier,
693 P.: Phytoplankton assemblages along the GEOVIDE section (GEOTRACES section GA01) using
694 CHEMTAX, in prep.
695
696 Tonnard, M., Planquette, H., Bowie, A. R., van der Merwe, P., Gallinari, M., de Gesincourt, F. D.,
697 Germain, Y., Gourain, A., Benetti, M., Reverdin, G., Treguer, P., Boutorh, J., Cheize, M.,
698 Barraqueta, J.-L. M., Pereira-Contreira, L., Shelley, R., Lherminier, P. and Sarthou, G.: Dissolved
699 iron in the North Atlantic Ocean and Labrador Sea along the GEOVIDE section (GEOTRACES
700 section GA01), Biogeosciences, in review.
701
702 Towler, P.: Radionuclides measured on water bottle samples during FRANKLIN cruise FR05/92,
703 PANGAEA, 2003.
704
705 Towler, P.: Radionuclides measured on water bottle samples during FRANKLIN cruise FR08/93,
706 PANGAEA, 2013.
707
708 Walsh, I. D. and Gardner, W. D.: A comparison of aggregate profiles with sediment trap fluxes,
709 Deep Sea Research Part A. Oceanographic Research Papers, 39, 1817-1834, 1992.
710
711 Wei, C., Lin, S., Wen, L. and Sheu, D. D. D.: Geochemical behavior of 210Pb and 210Po in the
712 nearshore waters off western Taiwan, Marine Pollution Bulletin, 64, 214-220, 2012.
713
714 Wei, C. L., Yi, M. C., Lin, S. Y., Wen, L. S. and Lee, W. H.: Seasonal distributions and fluxes of
715 210Pb and 210Po in the northern South China Sea, Biogeosciences, 11, 6813-6826, 2014.
716
717

718

719

Biogeosciences Discuss., https://doi.org/10.5194/bg-2018-210
Manuscript under review for journal Biogeosciences
Discussion started: 15 May 2018

720

721 Table 1. Biological characteristics of the water column determined by chlorophyll-a
722 concentration (8-day composite) from Fig. 4, including the date when the last bloom began,
723 the difference in chlorophyll-a concentration between the sampling time and last bloom peak,
724 and the days since the last bloom. Activity ratios of $^{210}Po_p/^{210}Pb_p < 1$ and their corresponding
725 depths are also shown. *NA* indicates that all samples from the corresponding depth range had
726 $^{210}Po_p/^{210}Pb_p$ equal to or greater than 1 (no sample with $^{210}Po_p/^{210}Pb_p < 1$).

Station	Sampling date	The date last bloom began	Last bloom peak-current state	Days since last bloom	$^{210}Po_p/^{210}Pb_p < 1$	
					0-100 m	> 100 m
1	5/19/14	3/6/14	Large	74	*NA*	Yes (120, 250, 500 m)
13	5/24/14	4/7/14	Small	47	Yes (60 m)	*NA*
21	5/31/14	4/7/14	Large	54	*NA*	Yes (120 m)
26	6/4/14	4/15/14	Large	50	*NA*	Yes (400 m)
32	6/7/14	5/9/14	Small	29	*NA*	*NA*
38	6/10/14	5/17/14	Small	24	Yes (60 m)	*NA*
44	6/13/14	5/9/14	Small	35	*NA*	*NA*
60	6/18/14	5/17/14	Large	32	*NA*	*NA*
64	6/19/14	5/17/14	Small	33	Yes (30 m)	*NA*
69	6/22/14	5/25/14	Small	28	Yes (20, 30 m)	*NA*
77	6/26/14	5/25/14	Small	32	Yes (10, 20, 50 m)	*NA*

727

728 Table 2. Global compilation of total particulate $^{210}Po/^{210}Pb$ activity ratios ($^{210}Po_p/^{210}Pb_p$) in the upper 200 m including this study.

Region		Sampling Method	Date	Size (μm)	Depth (m)	$^{210}Po_p/^{210}Pb_p$	Reference
Arctic	CESAR	*In-situ* pump	Apr – May 83	> 0.45	2-200	1.2	(Moore and Smith 1986)
	Arctic (ARK-XXII/2)	Niskin bottle	Jul-Sep 07	> 0.45	10-200	0.5	(Friedrich 2011)
	Chukchi Shelf	Niskin bottle	Jul-Sep 10	> 0.45	0-90	0.4	(He et al., 2015)
Atlantic	F.S. Meteor	Niskin bottle	Nov-Dec 73	> 0.4	0-200	3.1	(Bacon 1977)
	Cariaco Trench	Niskin bottle	Dec 73	> 0.4	0-200	1.8	(Bacon et al., 1980a)
	Labrador (R/V Knorr)	Niskin bottle	Jun 75	> 0.4	0-100	3.9	(Bacon et al., 1980b)
	South of New England	Niskin bottle	Jul 80	> 0.45	4-200	1.8	(Bacon et al., 1988)
	N. Atlantic (BOFS)	Niskin bottle	May-Jun 89, 90	> 0.45	0-150	5.1	(BODC et al., 2016)
	South-equa. Atlantic	Niskin bottle	May-Jun 96	> 0.7	10-200	1.7	(Sarin et al., 1999)
	BATS	Go-Flo bottle	Oct 96	> 0.45	0-200	3.7	(Kim and Church 2001)
	N. Atlantic (GA03)	*In-situ* pump	Oct-Nov 10, Nov-Dec 11	> 0.8	30-200	1.5	(Rigaud et al., 2015)
	N. Atlantic (GA01)	*In-situ* pump	May-Jun 14	> 1	8-200	1.4	This study
Pacific	North Pacific	Niskin bottle	Nov 73	> 0.4	10-150	8.5	(Bacon et al., 1976)
	W. Pacific (FR05/92)	Niskin bottle	Jul 92	> 0.45	0-200	1.3	(Towler 2003)
	Equa. Pacific	Go-Flo bottle	Aug-Sept 92	> 0.45 or 0.5	0-200	5.1	(Murray et al., 2005)
	W. Pacific (FR08/93)	Niskin bottle	Nov 93	> 0.45	0-200	15.7	(Towler 2013)
	W. Pacific (FR07/97)	Niskin bottle	Aug 97	> 0.45	0-200	7.2	(Peck and Smith 2002)
	Aleutian Basin	Niskin bottle	Jul-Aug 08	> 0.2	0-200	1.9	(Hu et al., 2014)
	E. Pacific (GP16)	*In-situ* pump	Oct-Dec 13	> 1	15-200	2.4	unpublished
Antarctic	S. Ocean (ANT-X/6)	Niskin bottle	Oct-Nov 92	> 0.45	20-200	3	(Smetacek et al., 1997)
	Bellingshausen Sea	Go-Flo bottle	Nov-Dec 92	> 0.45	0-100	13.9	(Shimmield et al., 1995)
	S. Ocean (ANT-XXIV/3)	Niskin bottle	Feb - Apr 08	> 0.45	25-200	1.3	(Friedrich et al., 2011)
	S. China Sea	Go-Flo bottle	Jan-Oct 07, May 08	> 0.45	0-200	1.7	(Wei et al., 2014)

Biogeosciences Discuss., https://doi.org/10.5194/bg-2018-210
Manuscript under review for journal Biogeosciences
Discussion started: 15 May 2018

	W. Taiwan	Go-Flo bottle	Apr 07	> 0.45	8-25	0.8	(Wei et al., 2012)
Margin Sea	Yellow Sea	Niskin bottle	Feb 93	> 0.7	0-100	0.9	(Hong et al., 1999)
	Mediterranean Sea	Sediment trap	Mar-Jun 03		200	4.5	(Stewart et al., 2007)

729

730

731

Biogeosciences Discuss., https://doi.org/10.5194/bg-2018-210
Manuscript under review for journal Biogeosciences
Discussion started: 15 May 2018

Biogeosciences Discuss., https://doi.org/10.5194/bg-2018-210
Manuscript under review for journal Biogeosciences
Discussion started: 15 May 2018

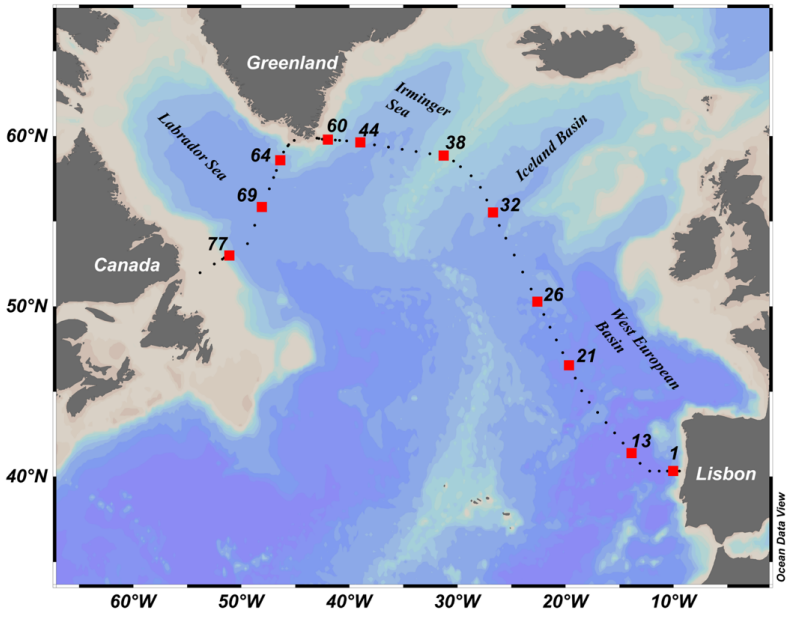

Fig. 1. Map of the GEOVIDE cruise track (black dots) and the 11 stations sampled for ^{210}Po and ^{210}Pb activity (red squares). Each sampling location is labeled with a station number. The sampling stations are divided into 4 regions (from east to west): West European Basin (stations 1, 13, 21, 26), Iceland Basin (stations 32, 38), Irminger Sea (stations 44, 60), and Labrador Sea (stations 64, 69, 77).

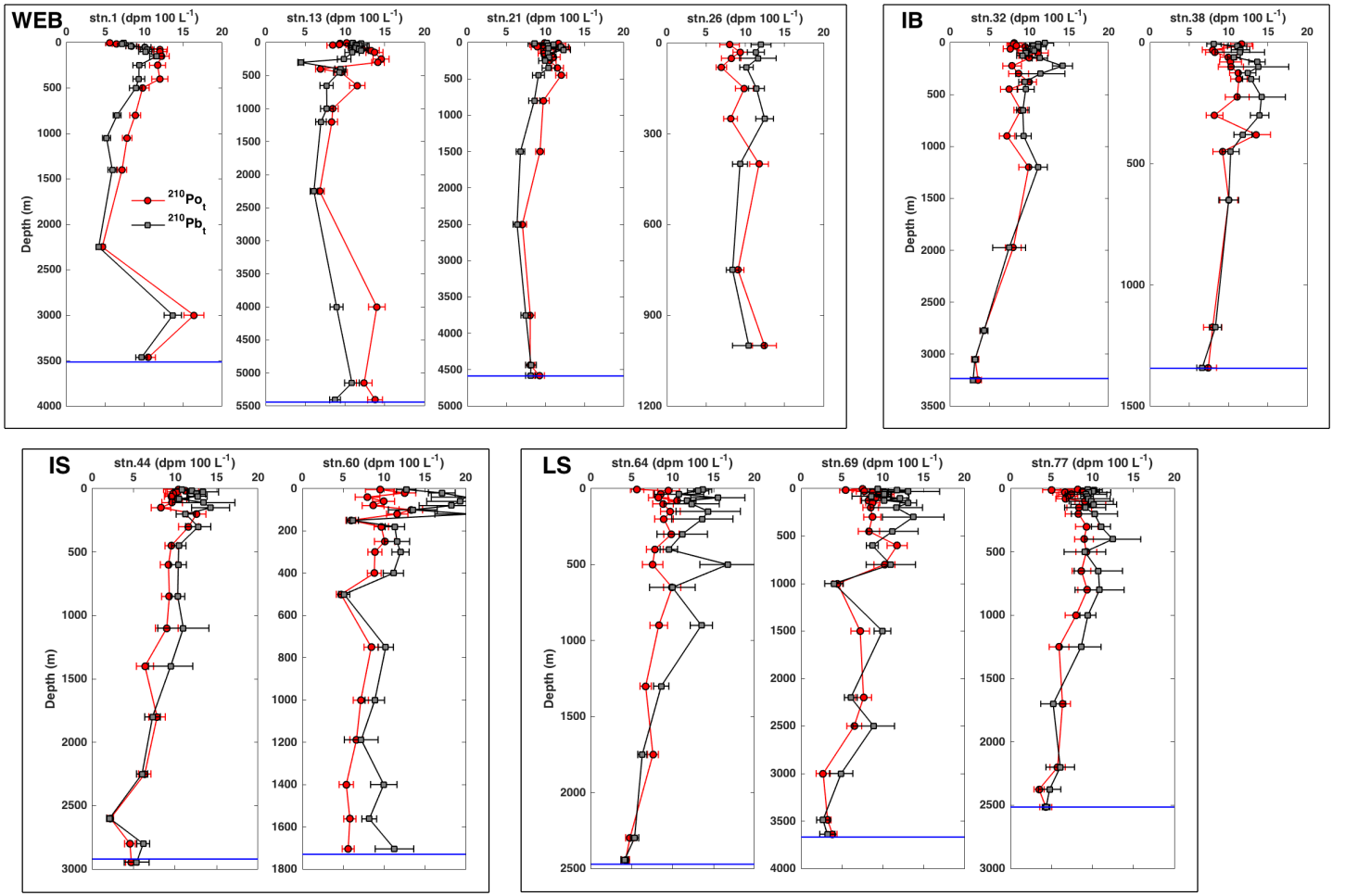

Fig. 2. The depth profiles of total ^{210}Po (^{210}Po$_t$, red circles) and ^{210}Pb activities (^{210}Pb$_t$, grey squares) along GEOVIDE section. The horizontal blue line is the bottom depth, which coincided with the deepest water sample except for station 26 which was sampled only

Biogeosciences Discuss., https://doi.org/10.5194/bg-2018-210
Manuscript under review for journal Biogeosciences
Discussion started: 15 May 2018

down to 1000 m. Note that the depth scale for each plot may be different. The profiles are shown in the order of sampling date with the region indicated on the top left of each box: Western European Basin (WEB), Iceland Basin (IB), Irminger Sea (IS), Labrador Sea (LS).

Biogeosciences Discuss., https://doi.org/10.5194/bg-2018-210
Manuscript under review for journal Biogeosciences
Discussion started: 15 May 2018

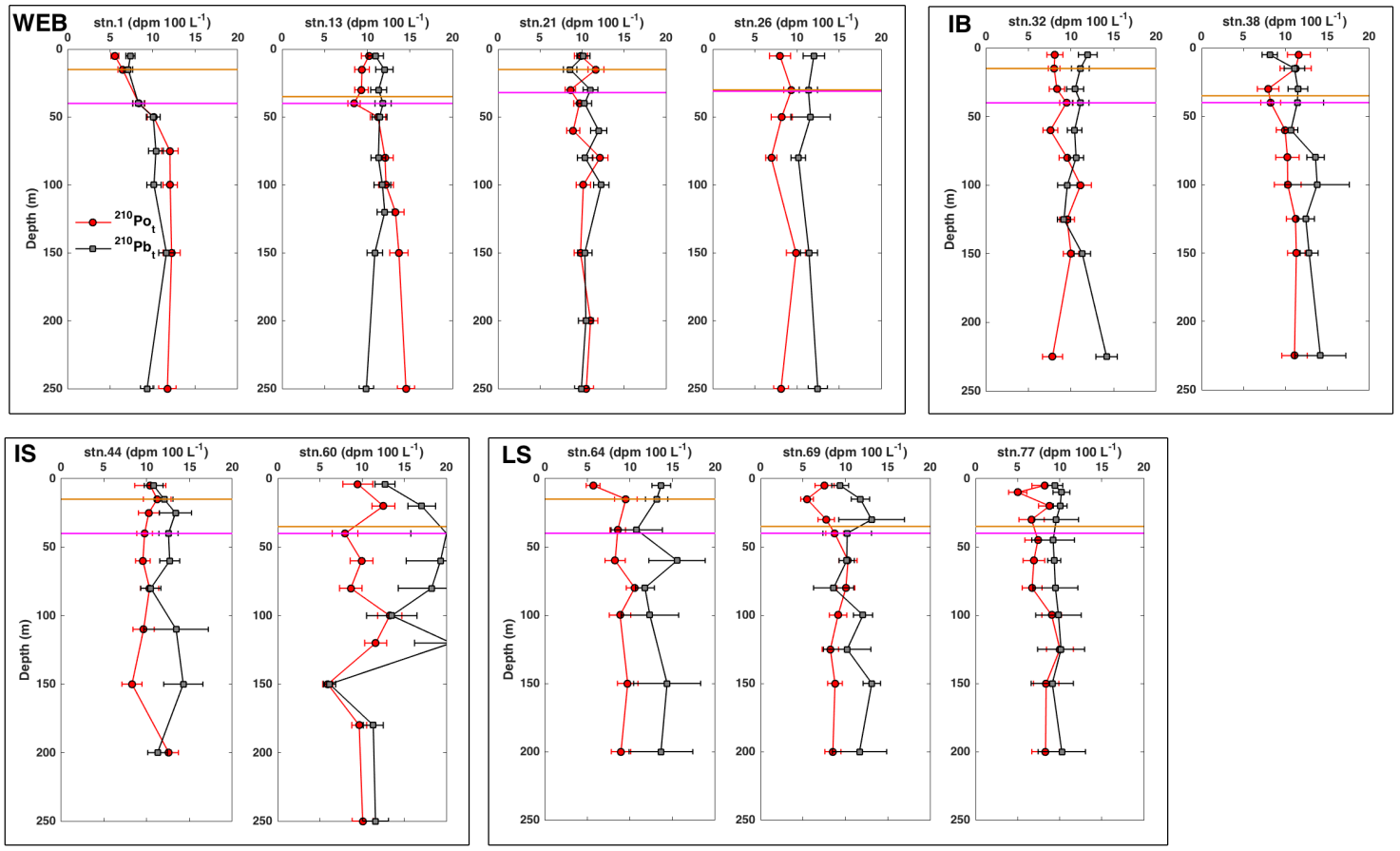

Fig. 3. A closer look at only the zoom for the upper 250 m of the depth profiles of total ^{210}Po (^{210}Po$_t$, red circles) and ^{210}Pb activities (^{210}Pb$_t$, grey squares) along the GEOVIDE section. The horizontal orange and magenta lines denote the mixed layer depth (MLD) and

Biogeosciences Discuss., https://doi.org/10.5194/bg-2018-210
Manuscript under review for journal Biogeosciences
Discussion started: 15 May 2018

Biogeosciences Discuss., https://doi.org/10.5194/bg-2018-210
Manuscript under review for journal Biogeosciences
Discussion started: 15 May 2018

the base of the euphotic zone ($Z_{1\%}$), respectively. The depth profiles are shown in the order of sampling and grouped by region (refer to Fig. 2 for the text abbreviations).

Biogeosciences Discuss., https://doi.org/10.5194/bg-2018-210
Manuscript under review for journal Biogeosciences
Discussion started: 15 May 2018

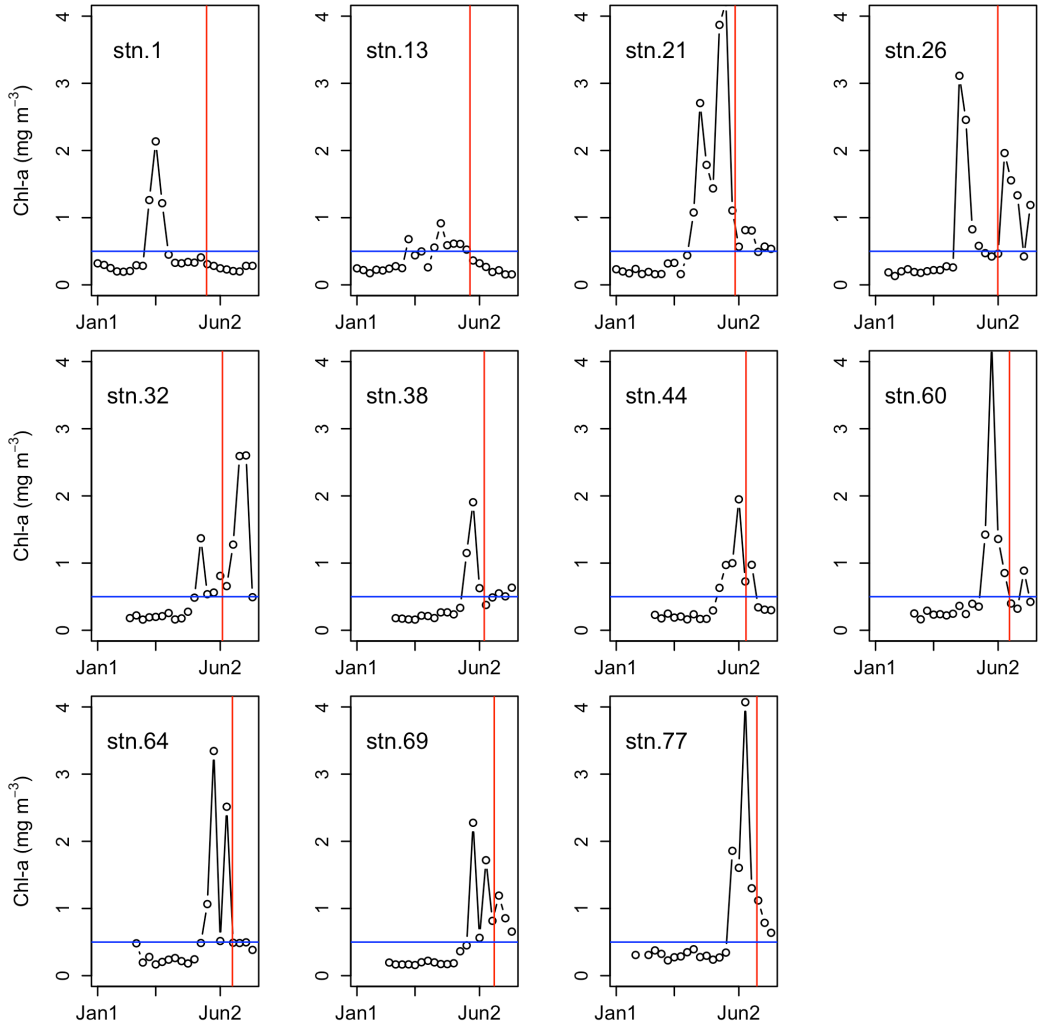

Fig. 4. Time-series (January 1 – July 12, 2014) chlorophyll-a concentrations (8-day averages) from Aqua MODIS (https://oceancolor.gsfc.nasa.gov) at each station along the GA01 transect. The vertical red line denotes the sampling date at each station. The horizontal blue line denotes chlorophyll-a concentration of 0.5 mg m^{-3}. The time when chlorophyll-a concentration first exceeded 0.5 mg m^{-3} after the end of the last bloom defines the date the next bloom began.

Biogeosciences Discuss., https://doi.org/10.5194/bg-2018-210
Manuscript under review for journal Biogeosciences
Discussion started: 15 May 2018

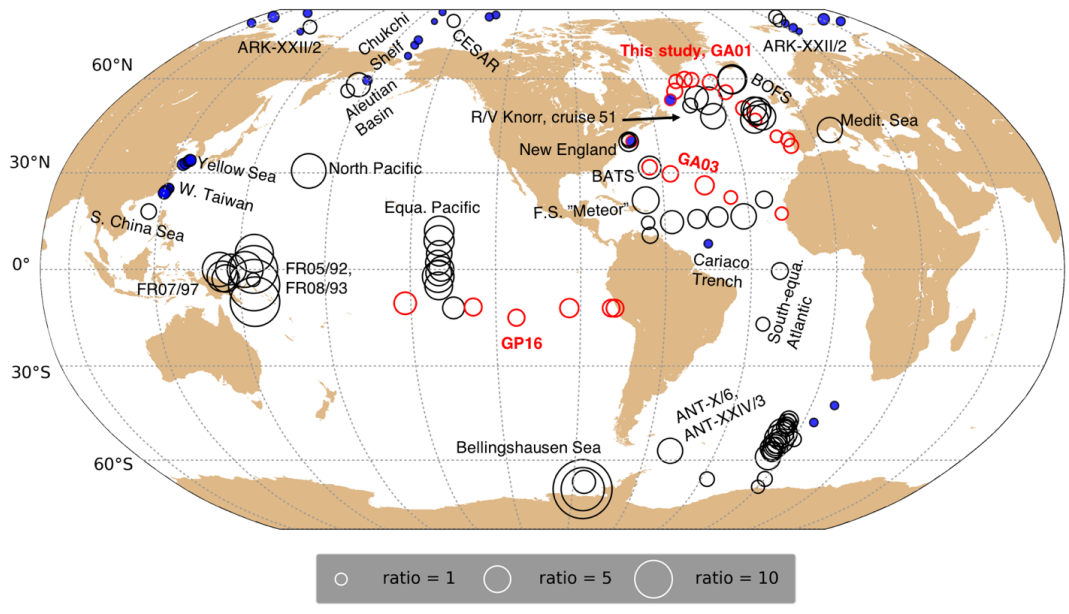

Fig. 5. Comparison of particulate $^{210}Po/^{210}Pb$ activity ratios in the upper 200 m from this study and 20 previous studies (references in Table 2). Information about the study site, sampling date, method, and particle size of each study are shown in Table 2. The black circles represent data from previous studies while the red circles are the results from samples analyzed in the Stewart lab from three recent GEOTRACES transects (GA03, GP16, and this study, GA01 GEOVIDE). The filled blue and open circles indicate activity ratios lower and higher than 1, respectively.

Biogeosciences Discuss., https://doi.org/10.5194/bg-2018-210
Manuscript under review for journal Biogeosciences
Discussion started: 15 May 2018

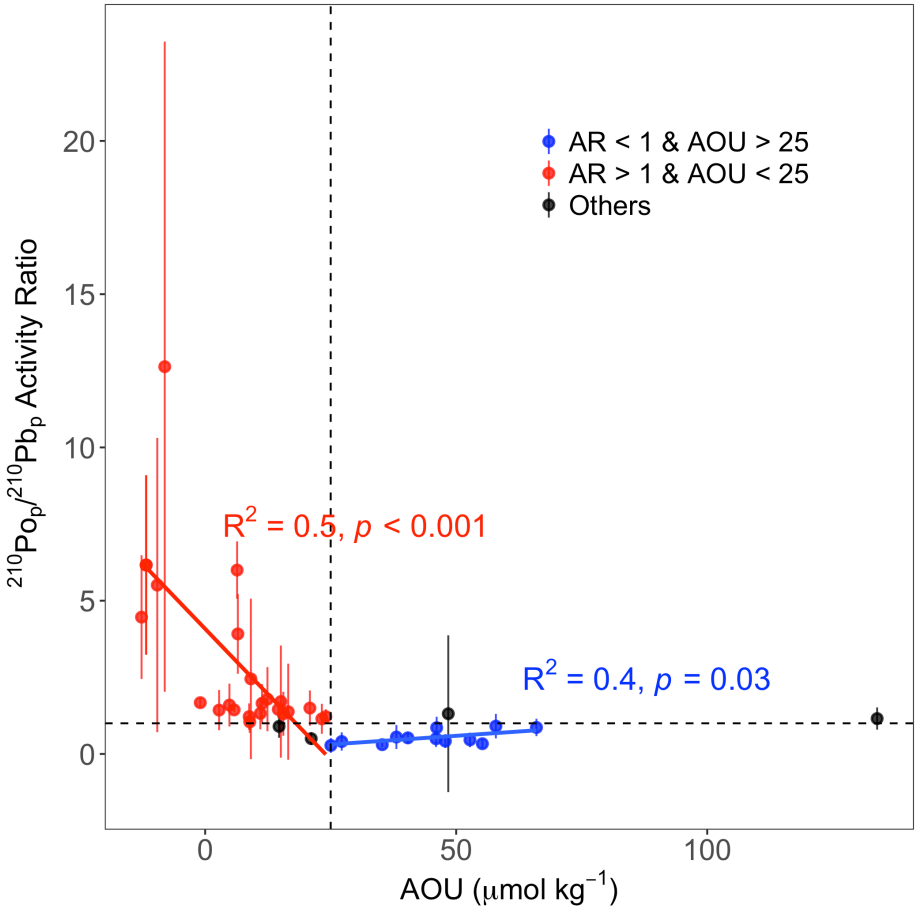

Fig. 6. The relationship between AOU (µmol kg^{-1}) and total particulate ^{210}Po/^{210}Pb activity ratio ($^{210}Po_p/^{210}Pb_p$) from the upper 200 m in the northern hemisphere (> 22 ºN) investigated by a linear regression model (red and blue lines). The 40 stations include data from previous studies, ARK-XXII/2 (77.38-87.83 ºN, n = 15) in the Arctic, BOFS (48.89-49.87 ºN, n = 7), GA03 (22.38-39.70 ºN, n = 7), and this study, GA01 (40.33-59.80 ºN, n = 11) in the North Atlantic. The horizontal dashed line represents $^{210}Po_p/^{210}Pb_p$ AR = 1 and the vertical dashed line represents AOU = 25 µmol kg^{-1}. Red circles denote the average $^{210}Po_p/^{210}Pb_p$ >1 and AOU < 25 µmol kg^{-1}, while blue circles denote the average $^{210}Po_p/^{210}Pb_p$ < 1 and AOU > 25 µmol kg^{-1}. Data that are in neither category are denoted by the black circles.

Biogeosciences Discuss., https://doi.org/10.5194/bg-2018-210
Manuscript under review for journal Biogeosciences
Discussion started: 15 May 2018

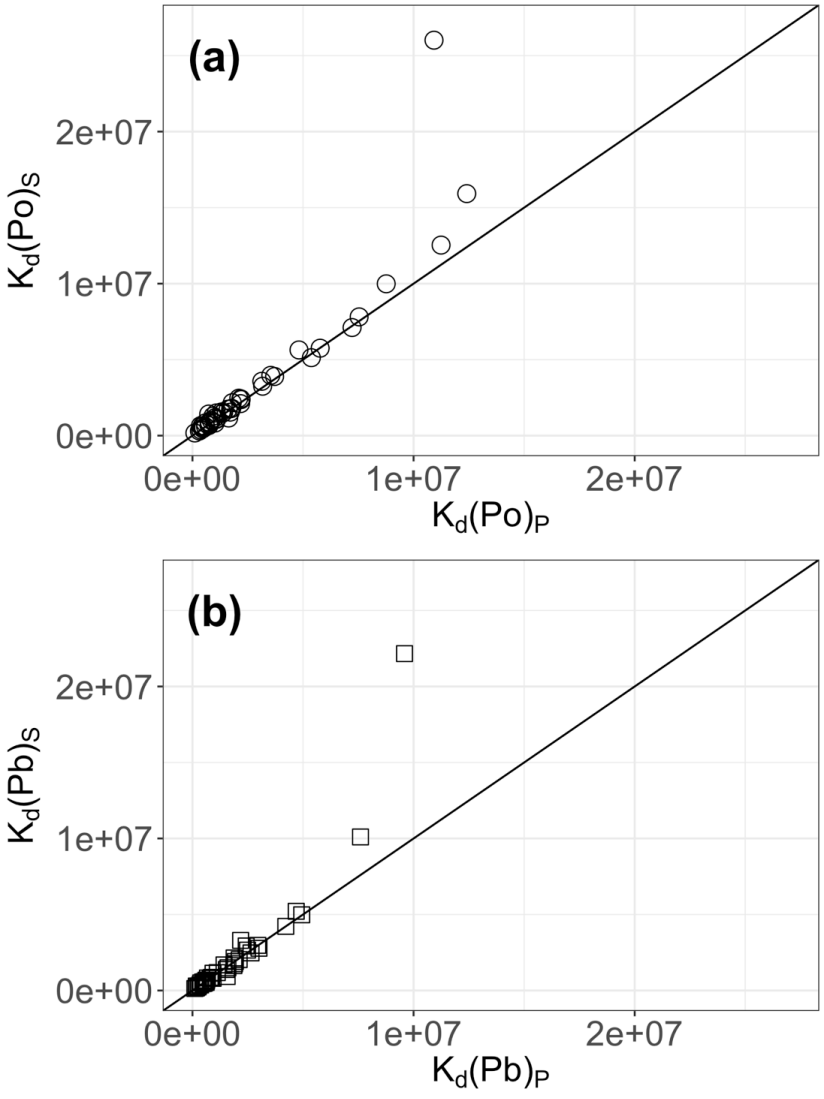

778

779 Fig. 7. Comparison of the partitioning coefficient (K_d) between the dissolved and small
780 particulate phases (K_{ds}) vs. between the dissolved and total particulate phases (K_{dp}) for (a)
781 ^{210}Po and (b) ^{210}Pb. The 1:1 line is indicated as the solid line in each plot.